A Method to Find the Viscous Damping Coefficient And a Faster Diagnostic Model

Michael Bastian — Shell Offshore Inc.
James Keating — Texas A&M University
Dr. J. W. Jennings — Texas A&M University

ABSTRACT

Several methods of calculating downhole dynamometer cards from surface dynamometer cards have been presented in the literature. Each of the methods requires knowing the viscous damping coefficient. This paper presents a non-iterative method for finding this term. A new method for calculating a downhole dynamometer card is also presented. This method is faster and more accurate than the fourier analysis and the finite difference method using the second order damped wave equation.

In Gibb's patent[1], two methods of determining the damping coefficient are presented. One is empirically based and the other is an equation that requires knowledge of the pump horsepower. But to calculate the pump horsepower the damping coefficient must be known. Therefore, an iterative procedure is required. This paper presents a non-iterative method for calculating the viscous damping coefficient. An improvement of the method presented by Everitt[2] is suggested and comments on variable damping are made.

A coupled set of first order linear differential equations is solved using finite differences to obtain a pump card. A cyclic boundary condition called the wrap around is used to eliminate problems associated with the end points. The wrap around condition eliminates iterating and allows for direct solution.

DAMPING COEFFICIENT

Importance

The intent of this section is to present a method derived for calculating the damping coefficient of the damped wave equation. The damping term is necessary to accurately calculate the forces and displacements down the rod string. The character of both the surface and downhole dynamometer cards is greatly affected by damping. An incorrect damping term could result in an erroneous diagnosis.

Damping in a sucker rod string results from a combination of many factors. In this study, the assumption is made that all of the real damping forces can be treated by using the viscous damping term. For this to be true an equivalent amount of energy must be removed by the viscous damping term as is removed by the actual forces.

Previous Work

In Gibb's patent, two techniques for determining the damping coefficient were presented. One method was empirically based on field damping measurements. In the other technique, Gibbs assumed the integrated average velocity of the sucker rod is equivalent to the root mean square velocity of the polished rod in simple harmonic motion. Using this assumption, an equation to calculate the damping term was presented. In Everitt's thesis, a similar equation was presented to calculate the damping term with variable density rods. This equation is:

$$c = \frac{(550)(144g_c)}{\sqrt{2}\pi}\frac{(PRHP - HP_{hyd})T^2}{(\sum \rho_i A_i X_i)S^2} \qquad \ldots(1)$$

As Everitt pointed out, the hydraulic horsepower must be known to calculate the damping coefficient. Hydraulic horsepower can be calculated from:

$$HP_{hyd} = 7.36E-06 \quad Q \quad SG \quad L_n \qquad \ldots(2)$$

where the production rate at the pump, Q, is given by:

$$Q = .1484 \quad A_p \quad S_n \quad SPM \quad E_p \qquad \ldots(3)$$

To calculate the production at the pump the stroke length at the pump is needed. The stroke length comes from the pump card. To calculate the pump card the damping coefficient is needed. Therefore, the algorithm presented by Everitt involved an iterative process to determine the damping coefficient.

Methods Developed

A non-iterative technique for finding the viscous damping coefficient is presented next. An improvement of Everitt's method is suggested and comments on variable damping are made.

Curve Generation

The work performed at the pump is the movement of fluids through the pump. Hydraulic horsepower is defined by K. E. Brown[3] as the "power required to lift a given volume of fluid vertically, through a given distance in a given period of time". Using Equations (2) and (3) the hydraulic horsepower is calculated.

Work is also defined when a force causes a displacement. Power is defined as the amount of work per unit time. The power at the pump can be obtained by integrating the downhole dynamometer card. This integration is a summation of the forces and displacements at the pump for a complete pumping cycle.

The viscous damping term is assumed to account for all energy dissipation in the system. If there were no energy losses the area of the surface card would equal the area of the downhole card. For a sucker rod system at a given time there normally is a power loss from the surface to the pump. This means there is a unique damping term for that system and time. If a damping term is used that is smaller than the actual damping, the effect is to add power to the system. If the damping term used is larger than the actual damping, then too much power is being removed from the system.

The effect of increasing or decreasing the damping term on the area of the card is dramatic. The effect of varying the damping term on the stroke length is not very significant. With this in mind, it is possible to calculate the pump horsepower by two different methods. The first method is to integrate the area of the pump card to obtain a pump horsepower. The second method is to use the stroke length to calculate the pump flow rate. With the flow rate, the hydraulic horsepower can be calculated from Equation (2). By varying the damping coefficient and calculating the resultant pump horsepower by each method, a plot of pump horsepowers versus the damping coefficient is generated.

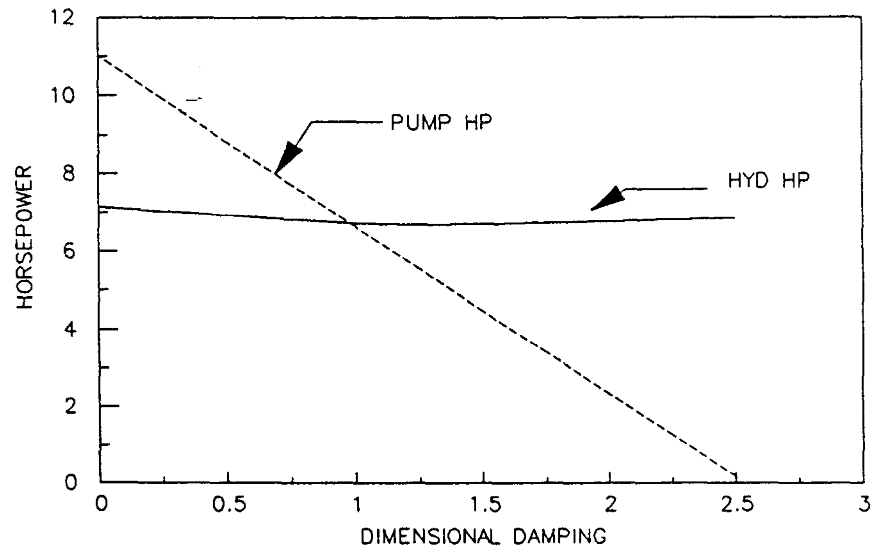

Figure 1 - Solution for the Damping Coefficient

By definition, the damping coefficient where the two curves intersect is the correct one. A simple algorithm was developed to find the point where the curves cross. The validation of this method is presented later.

Node Velocities

The method presented by Gibbs and Everitt to calculate the damping coefficient involved using an average velocity. An expression for the average velocity was obtained by assuming simple harmonic motion for the polished rod. This velocity was then assumed to be equivalent to the root mean square velocity.

In the solution presented in this work, the velocities at each node for each time in the cycle are calculated. Therefore, an average velocity can be found for the rod string during a complete period. This average velocity can then be used in Equation (1) in place of the root mean square velocity to calculate the damping coefficient.

$$c = \frac{(550)(144g_c)(PRHP - HP_{hyd})T}{(\sum \rho_i A_i X_i)S} v_{(node\ averaged)} \qquad \ldots(4)$$

To check the validity of the calculation procedure, data generated from a design model with a known damping coefficient was run on the diagnostic model presented in this work. The damping coefficient used to generate the data was input as the correct value in the diagnostic model. The damping coefficient was then calculated from Equation (4). The damping coefficient calculated was within 1% of the actual value. Using the actual node averaged velocities improves the method presented by Everitt.

Up & Down Damping

In several of Gibbs' papers covering his diagnostic and predictive programs, the ability to vary the damping coefficient on the upstroke and downstroke is mentioned. This topic has been discussed but no formal presentation in the literature was found. A predictive model was modified to allow for varying the damping coefficient on the upstroke and downstroke. Using the surface card generated from this model as input, attempts were made to calculate the damping coefficients. The velocities were averaged for the upstroke and the downstroke, and used in a modified Equation (4). A problem in splitting the upstroke and downstroke at the pump prevented obtaining satisfactory results with this method.

An attempt was made to use the curve generation technique to solve for the upstroke and downstroke damping coefficient. However, accurately splitting the horsepower at the pump into upstroke and downstroke values prevented adequate solutions.

During the attempts to calcuate upstroke and downstroke damping coefficients, a problem was identified with using iterative techniques to find the solution. Figure 2 illustrates this problem.

Each line on Figure 2 represents the pump horsepower corresponding to a set of upstroke and downstroke damping coefficients. An infinite number of lines could be generated which would form a surface of damping coefficients for various pump horsepower's. Regardless of what the damping coefficient actually is, a finite amount of horsepower is delivered to the pump on each pumping cycle. For any given horsepower, there is an infinite combination of upstroke and downstroke damping coefficients that will give that horsepower. It would be possible to converge on several possible combinations of damping coefficients using an iterative technique. A further constraint is needed to enable calculation of up and downstroke damping. More work is needed to further define the concept of variable damping.

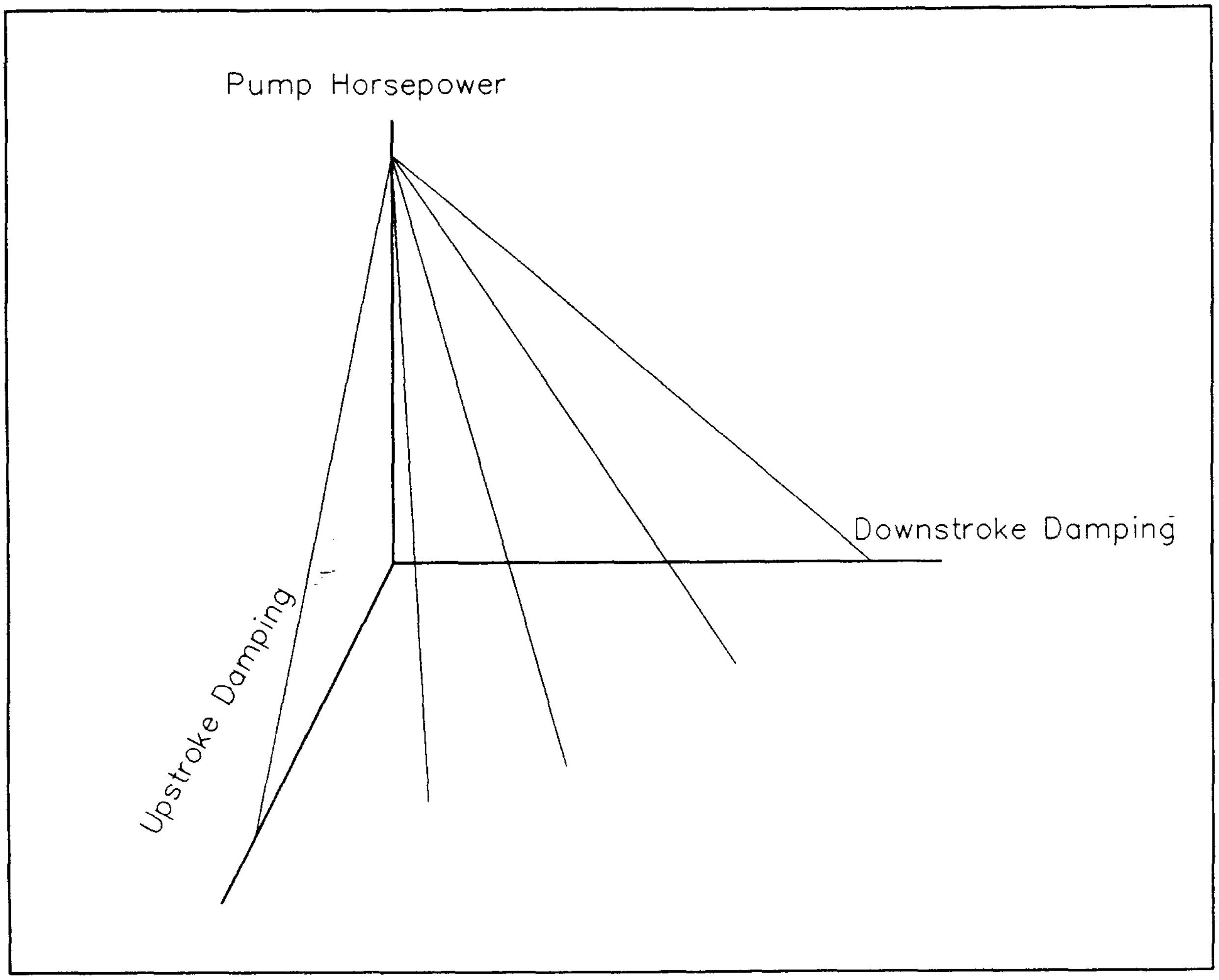

Figure 2 - Up & Down Damping Curves

TWO EQUATION DIAGNOSTIC MODEL

Formulation of Reduced Order Differential Equations

The one dimensional damped wave equation is a second order linear hyperbolic differential equation which describes the longitudinal vibrations in a long uniform rod. This equation, with the proper boundary conditions, can be used to describe the motion of a sucker rod string. From a description of the physical system (a sucker rod string), a set of coupled first-order linear differential equations can be derived. By reducing the order of the differential equation, solution times are accelerated.

Using a free body diagram as shown in Figure 3 and Newton's second law, an analysis of the forces acting on the sucker rods is performed.

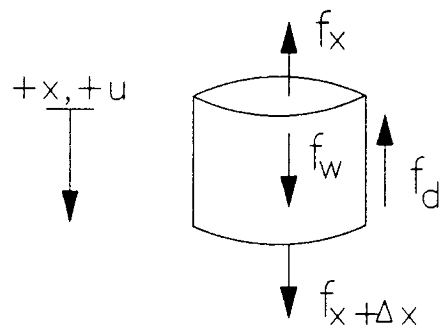

Figure 3 - Free Body Diagram

From Newton's second law, $\sum f = ma$:

$$f_{x+\Delta x} - f_x - f_D + f_W = m\frac{\partial v}{\partial t} \qquad \ldots(5)$$

The force f_x and $f_{(x+\Delta x)}$ are tension forces in the directions shown. The force due to the weight of the rod element is f_W. The viscous damping force is given by f_D. The force due to the weight of the rods can be expressed as the mass times the acceleration from gravity. Rewriting the mass of the rods as,

$$m = \frac{\rho A_r \Delta x}{144 g_c} \qquad \ldots(6)$$

and substituting into Equation (2) gives:

$$f_{x+\Delta x} - f_x - f_D + \frac{\rho A_r \Delta x g}{144 g_c} = \frac{\rho A_r \Delta x}{144 g_c}\frac{\partial v}{\partial t} \qquad \ldots(7)$$

The viscous damping force is used to describe the effects of lost energy. Doty and Schmidt[4] showed that other forces dissipated energy. However, by assuming the dissipation is due to viscous damping, non-linearities are avoided in the differential equation. In field practice this assumption has proved adequate.

C.E. Crede[5] defines viscous damping as "the dissipation of energy that occurs when a particle in a vibrating system is resisted by a force that has a magnitude proportional to the magnitude of the velocity of the particle and direction opposite to the direction of the particle." Therefore, the damping force is proportional to the velocity of the rod. Gibb's presented a damping term in his patent that is dimensionally consistent and when multiplied by the velocity of the rod approximates the viscous damping effects. This term is given by:

$$c = \frac{\pi a \nu}{2L} \qquad \ldots(8)$$

where

$$\nu = \frac{4.42E-02L(PRHP-HP_{hyd})T^2}{(\sum A_i X_i)S^2} \qquad \ldots(9)$$

Using the definition of viscous damping and Gibb's damping term, the viscous damping force is written as:

$$f_D = c\Delta x \frac{\rho A_r}{144g_c}\frac{\partial u}{\partial t} \qquad \ldots(10)$$

Substituting Equation (10) into Equation (7) gives:

$$f_{x+\Delta x} - f_x - c\Delta x \frac{\rho A_r}{144g_c}\frac{\partial u}{\partial t} + \rho A_r \Delta x \frac{g}{144g_c} = \rho \frac{A_r \Delta x}{144g_c}\frac{\partial \nu}{\partial t} \qquad \ldots(11)$$

The definition of the first forward difference of F at x is:

$$F_x = \frac{f_{x+\Delta x} - f_x}{\Delta x} \qquad \ldots(12)$$

By definition the first forward difference is an approximation of the first derivative of the function with some associated error. For purposes of this work the finite difference error will be dropped from the derivation of the equations. Dividing equation 8 by Δx gives:

$$F_x - c\frac{\rho A_r}{144g_c}\nu + \frac{\rho A_r g}{144g_c} = \rho \frac{A_r x}{144g_c}\nu_t \qquad \ldots(13)$$

Equation (13) is one of the partial differential equations that will be coupled to solve for the pump dynamometer card. The term

$$\frac{\rho A_r g}{144g_c}$$

is the static weight of the rods. Since this term is constant, its effects can be dropped at this point of the derivation and superimposed on the final calculated forces. Equation (13) can then be written as:

$$F_x - c\frac{\rho A_r}{144g_c}\nu = \rho \frac{A_r x}{144g_c}\nu_t \qquad \ldots(14)$$

The second equation is derived using Hooke's Law:

$$f = E A_r \frac{\partial u}{\partial x} \qquad \ldots(15)$$

Differentiating this equation with respect to time yields the following:

$$F_t = E A_r \frac{\partial^2 u}{\partial t \partial x} \qquad \ldots(16)$$

Recognizing that

$$\frac{\partial^2 u}{\partial t \partial x}$$

is equal to

$$v_x$$

the second equation of the coupled set is:

$$F_t = E A_r v_x \qquad \ldots(17)$$

Equations (14) and (17) when coupled together represent the system of first order differential equations needed to solve the problem. Using these two equations and the proper boundary conditions allows for direct calculation of the forces and velocities. Displacements are then found by integrating the velocities. These equations allow for variation in rod diameter and density. The equations are a reduced order form of the second order one dimensional damped wave equation.

Boundary Conditions

The task of solving these two first order linear differential equations involves starting from some condition in time and space and advancing the solution in space for all times. Each of the differential equations have two independent variables with respect to time and space. Therefore, to obtain a solution two boundary conditions and two initial conditions are ordinarily required. The two boundary conditions are provided by the surface dynamometer card and can be represented as:

$$F(0,t) \text{ and } u(0,t)$$

By arbitrarily setting the origin at the polished rod, the surface dynamometer card supplies a complete cycle of forces and displacements. Initial conditions are not required because only periodic solutions are considered. The assumption that the pumping unit is at steady state insures the derivatives of the forces and displacements with respect to time do not change from period to period.

Discrete Analogs

To implement these equations into a numerical algorithm suitable for computation on a digital computer, it is necessary to transform the continuous functions to discrete analogs using the methods of finite difference calculus. The derivations of finite difference analogs for derivatives of functions is well know and well documented in many excellent texts on numerical methods. The discretized form of equations (14) and (17) is given by the following equations:

$$f_{(i,j)} = f_{(i-1,j)} + \left[\frac{\rho A_r \Delta x}{144 g_c 2 \Delta t} \left(v_{(i,j+1)} - v_{(i,j-1)} \right) \right] + c \frac{\rho A_r}{144 g_c} v_{(i,j)} \quad \ldots(18)$$

$$v_{(i,j)} = \frac{\Delta x}{E A_r 2 \Delta t} \left[f_{(i-1,j+1)} - f_{(i-1,j-1)} \right] + v_{(i-1,j)} \quad \ldots(19)$$

Stability Criterion

Everitt, Knapp[6], and Hornbeck[7] show that for the undamped wave equation

$$a^2 \frac{\partial^2 u}{\partial x^2} = \frac{\partial^2 u}{\partial t^2} \quad \ldots(20)$$

the condition necessary for stability of the finite difference analog is:

$$\left[\frac{\Delta x}{a \Delta t} \right]^2 \leq 1 \quad \ldots(21)$$

A formal mathematical presentation of stability is not made. In practice, the algorithm has been shown stable when the criterion described above has been met. The velocity of force propagation a can be written as:

$$a = \sqrt{\left(144 E \frac{g_c}{\rho} \right)} \quad \ldots(23)$$

By substituting Equation (23) into Equation (21) the stability criterion can be expressed as:

$$\Delta t \geq \frac{\Delta x}{\sqrt{\left(144 E \frac{g_c}{\rho} \right)}} \quad \ldots(24)$$

Wrap Around Condition

A problem exists in handling the end points in Equations (18) and (19) when using central differences in time.

$$f_{(i,j)} = f_{(i-1,j)} + \left[\frac{\rho A_r \Delta x}{144 g_c 2 \Delta t} (v_{(i,j+1)} - v_{(i,j-1)}) \right] + c \frac{\rho A_r}{144 g_c} v_{(i,j)} \quad \ldots(18)$$

$$v_{(i,j)} = \frac{\Delta x}{E A_r 2 \Delta t} [f_{(i-1,j+1)} - f_{(i-1,j-1)}] + v_{(i-1,j)} \quad \ldots(19)$$

A surface dynamometer card provides the boundary conditions and is composed of force and displacement data for one cycle. The discrete points from the surface dynamometer card are numbered from 0 to N. However, when using central differences in time the points -1 and N+1 are needed at the respective endpoints. This problem is handled by wrapping the endpoints around. This condition can best be explained by Figure 4.

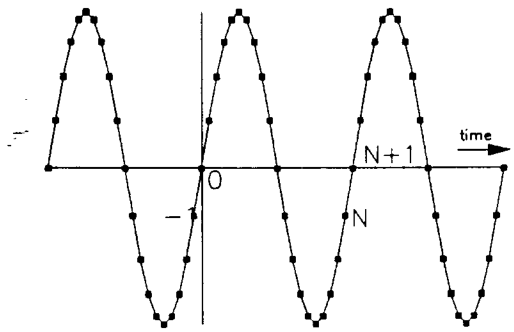

Figure 4 - The Wrap Around

where:

$$v(x,-1) = v(x,N) \qquad f(x,-1) = f(x,N)$$

$$v(x,N+1) = v(x,0) \qquad f(x,N+1) = f(x,0)$$

MODEL VALIDATION

The algorithms presented were programmed in Fortran 77 for use on personal computers. The resulting computer program can generate a pump dynamometer card when given a surface dynamometer card. The program handles various geometry pumping units, rod strings of different diameter and composition and can calculate the damping coefficient.

To test the validity of the algorithms and the resulting computer program, test cases were run and compared against other standards. These standards are a finite difference predictive model and a finite difference diagnostic model. The finite difference predictive model was originally presented by Gibbs.[8] The finite difference diagnostic model was presented by Everitt. The finite difference predictive model is referred to as PRED, Everitts diagnostic model is referred to as DCARD, and the finite difference diagnostic model presented in this work is referred to as DIAG.

Predictive Model Comparison

PRED is used to design new pumping unit installations. By inputting desired pumping unit dimensions, rod dimensions, and by defining a pump boundary condition the model generates a surface dynamometer card. The pump boundary conditions such as a full pump, loose anchor, or fluid pound define the shape of the pump dynamometer card. To validate DIAG using PRED, the following steps were taken:

1. Set a pump boundary condition and choose appropriate data for PRED and generate a surface dynamometer card.
2. Use the surface dynamometer card from PRED as input to DIAG to calculate the pump dynamometer card.
3. Compare the pump card from DIAG with the pump card from PRED.

By going through this procedure a "loop" is completed. You define a pump card and calculate a surface card from it. You then take the surface card and calculate the pump card. If the two pump cards are the same the mathematical models and computer programs can be considered valid. Test Case #1 is described in Table 1.

The assumption that the polished rods velocity is equal to 6% second simple harmonic motion alleviates the need for pumping unit dimensions when using PRED to test DIAG. Actual pumping unit kinematics were also used but showed very little difference. Figure 5 represents the surface card generated by PRED. Figure 6 is the comparison of the actual pump dynamometer card from PRED and the one calculated from DIAG. As can be seen the calculated pump card from DIAG compares excellently with the one from PRED.

Table 2 shows the data that was used to generate the surface card for Test Case #2. Figure 7 is the surface card for this data and Figure 8 is a comparison of the pump cards. Again, the match is good. Other pump conditions were tested with equally good results. An observation was made when testing DIAG using PRED as the input regarding the number of cycles and elements needed for convergence in PRED. Besides comparing the general shape and size of the pump dynamometer cards the area was also calculated for each and compared. It was observed that differences in area could be significant if large element sizes and few cycles were used. The element size used in PRED had to be less than 75 feet and the number of cycles greater than 10 for the differences in the area of the pump cards to be less than 1%. In general practice, this kind of accuracy would not be needed to do diagnostic work. However, it does become critical when calculating the damping coefficient.

Diagnostic Model Comparison

The finite difference model of this paper was compared to the finite difference model DCARD from T. A. Everitt's work. Everitt's model uses a discretized form of the second order damped wave equation to solve for the pump dynamometer card. In Everitt's thesis, he compared his model very favorably to an analytical model using the truncated Fourier Series similar to Gibb's original model. This model was presented by D. J. Schafer[9] and modified by J. W. Jennings.

The comparisons presented are from the field data that Everitt used to compare his model to the analytic model. Tables 3 through 6 describe the data sets. The surface and downhole dynamometer cards which correspond to these data sets are shown in Figures 9 through 16. DIAG compares excellently with DCARD in each of these cases. Though not tested, by inference DIAG should also compare well with the analytic method. One area of difference in each of the comparisons is at the upper left and lower right of each card. These corners represent the beginning of the upstroke and the beginning of the down stroke respectively. On each one of these cards DCARD has forces that extend beyond those calculated by DIAG. When using the second order damped wave equation to calculate displacements, the forces are calculated using Hooke's Law. The velocity term necessary for calculating the forces at the pump using Hooke's law is found using a second order backward difference. In DIAG the forces are calculated from the actual velocities at the pump. Therefore, DIAG's method is able to more accurately handle conditions at the corners.

Damping Coefficient Validation

The method presented to calculate the damping coefficient was tested using the predictive model. A surface card was created with a known damping coefficient. This surface card was then used as input into DIAG. By generating curves of pump horsepower defined by the area of the dynamometer card and hydraulic horsepower the correct damping coefficient is found. An example is presented in Figure 17.

The data used to generate these dynamometer cards is identical to Test Case #1. The damping coefficient calculated was accurate within 0.25%. The number of points used to create the curves in this example was 20. Using only three points the damping coefficient is calculated to within 2% of the actual value. A converged answer from the predictive model is essential to accurately calculate the damping coefficient. Element size needed to obtain a converged answer was between 50 and 75 feet. The number of cycles needed was between 10 & 15. In field practice this error is not introduced with an actual dynamometer card.

CONCLUSIONS

The following conclusions can be made as a result of this work:

1. By reducing the order of the second order damped wave equation a coupled set of first order differential equations is used to accurately solve for a pump dynamometer card.

2. When solving Equations (14) and (17) using finite differences, the end points can be accurately handled without additional iterations by using the cyclic boundary condition presented.

3. The viscous damping term used to account for energy dissipation can be accurately obtained using the curve generation technique presented.

4. When solving for different damping terms on the upstroke and downstroke, an infinite number of solutions is possible using iterative methods.

5. The predictive model requires rod lengths of 50 to 75 feet and 10 to 15 cycles to obtain a converged answer. This is apparent when solving for the damping coefficient using a surface card generated from the predictive model.

REFERENCES

1. Gibbs, S. G.: "Method of determining Sucker Rod Pump Performance," U.S. Patent No. 3,343,409 (Sept. 26,1967).

2. Everitt, T. A.: "An Improved Finite Difference Calculation of Downhole Dynamometer Cards for Sucker Rod Pumps," MS Thesis, Texas A&M University, College Station, Texas (Dec. 1987).

3. Brown, K. E.: *The Technology of Artificial Lift Methods*, Volume 2A, The Petroleum Publishing Company, Tulsa, Oklahoma (1980) 43.

4. Doty, D. R. and Schmidt, Z.: "An Improved Model for Sucker Rod Pumping", *Journal of Petroleum Technology*, (February, 1983) 33-41.

5. Crede, C. E.: *Shock and Vibration Concepts in Engineering Design*, Prentice-Hall Inc., Englewood Cliffs, New Jersey (1965) 138.

6. Knapp, R. M.: "A dynamic Investigation of Sucker-Rod Pumping," M.S. Thesis, University of Kansas, Topeka, Kansas (January, 1969).

7. Hornbeck, R. W. : *Numerical Methods*, Prentice-Hall, Inc., Englewood Cliffs, New Jersey, (1975) pp 16-34.

8. Gibbs, S. G.: "Predicting the Behavior of Sucker Rod Pumping Systems," Journal of Petroleum Technology, (July 1963) 769-778.

9. Schafer, D. J.: "An Investigation of Analytical and Numerical Sucker Rod Pumping Mathematical Models," M.S. Thesis, Texas A & M University, College Station, Texas (May 1987).

NOMENCLATURE

a - Velocity of force propagation in the rods, ft/sec

A_r - Rod cross-sectional area, in^2

A_p - Plunger cross-sectional area, in^2

c - Damping coefficient, sec^{-1}

E - Young's modulus of elasticity, psi

E_p - Pump efficiency, fraction

f - Tension force acting on rod elements, lbf

f_D - Damping force, lbf

f_w - Buoyant weight of rod element, lbf

g_c - Units conversion factor, (lbm-ft)/lbf-sec^2)

HP_{hyd} - Hydraulic horsepower, hp.

L - Total length of rod string, ft.

L_n - Fluid level or net lift, ft.

Q - Pump production rate, BPD

S - Polished rod stroke, ft.

SG - Specific gravity of fluid, fraction

S_n - Net pump stroke, in

SPM - Pumping speed, strokes/min

t - Time, sec

T - Period of pumping cycle, sec

u - Rod displacement, ft.

W_b - buoyant weight of total rod string, lbf

x - Axial distance along the rod string, ft.

v - Velocity of rod element, ft/sec.

ρ - Rod density, lbm/ft^3

Table 1
Description of Test Case #1

Rod Data

Diameter	Length (ft.)	Material	Elasticity
0.875	1690	Steel	30.5*E6
0.750	3310	Steel	30.5*E6

Downhole Data

Plunger Diameter:	1.5 in.	Pump Depth:	5000 ft.
Pumping Speed:	8 SPM	Fluid Level:	5000 ft.
Stroke Length:	54 in.	Fluid Gravity:	1.0
Pump Condition:	full pump		

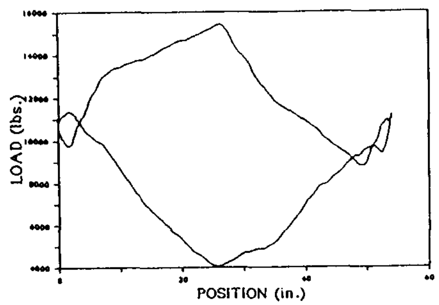

Figure 5 - Test Case #1 Surface Dynamometer Card

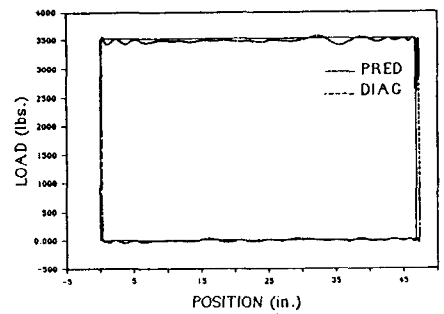

Figure 6 - PRED & DIAG for Test Case #1

Table 2
Description of Test Case #2

Rod Data

Diameter	Length (ft.)	Material	Elasticity
1.000	2000	Steel	30.5*E6
0.875	3000	Steel	30.5*E6
0.750	4000	Steel	30.5*E6

Downhole Data

Plunger Diameter:	1.5 in.	Pump Depth:	9000 ft.
Pumping Speed:	16 SPM	Fluid Level:	9000 ft.
Stroke Length	54 in.	Fluid Gravity:	0.9
Pump Condition:	full pump		

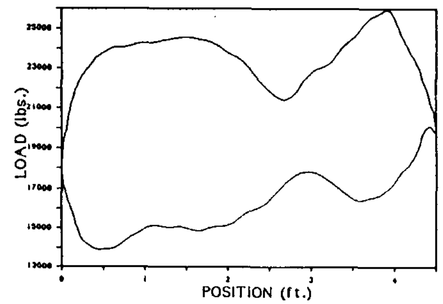

Figure 7 - Test Case #2 Surface Dynamometer Card

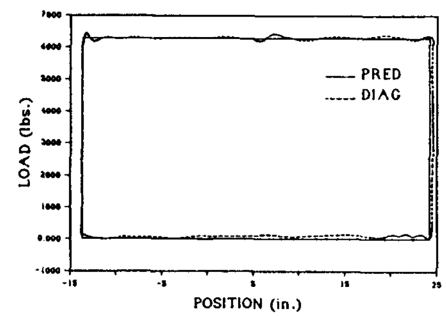

Figure 8 - PRED & DIAG for Test Case #2

Table 3
Description of Belcher #51
Rod Data

Diameter	Length (ft.)	Material	Elasticity
0.875	1500	Steel	30.5*E6
0.750	2400	Steel	30.5*E6

Downhole Data

Plunger Diameter:	1.5 in.	Pump Depth:	3900 ft.
Pumping Speed:	8 SPM	Fluid Level:	2850 ft.
Fluid Gravity:	0.92		

Pumping Unit Data

Unit Design.:	M-228-256-120	Stroke Length:	121 in.
Manufacturer:	Lufkin	Struc. Unbal.:	-3435
Rotation:	CCW	Phase Angle:	24 deg.

API Dimensions (in.):

R	A	C	I	K	P
33.125	312.0	258.0	186.0	244.7	173.75

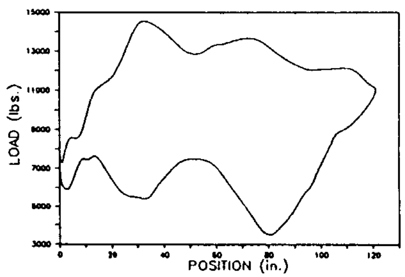

Figure 9 - Surface Dynamometer Card for Belcher #51

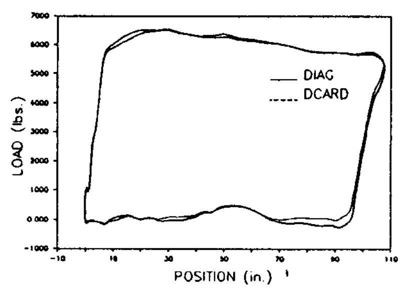

Figure 10 - DCARD & DIAG Cards for Belcher #51

Table 4
Description of Down #2
Rod Data

Diameter	Length (ft.)	Material	Elasticity
0.750	3179	Steel	30.5*E6

Downhole Data

Plunger Diameter:	1.5 in.	Pump Depth:	3234 ft.
Pumping Speed:	10 SPM	Fluid Level:	unknown
Fluid Gravity:	0.8		

Pumping Unit Data

Unit Design.:	C-114-143-64	Stroke Length:	64 in.
Manufacturer:	Lufkin	Struc. Unbal.:	360
Rotation:	CCW	Phase Angle:	0 deg.

API Dimensions (in.):

R	A	C	I	K	P
27.0	84.0	72.062	72.0	112.93	84.0

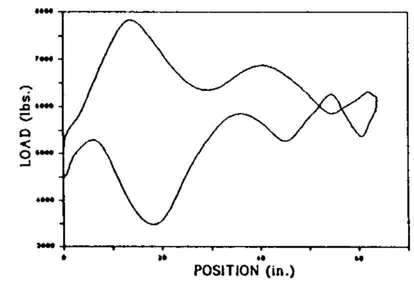

Figure 11 - Surface Dynamometer Card for Down #2

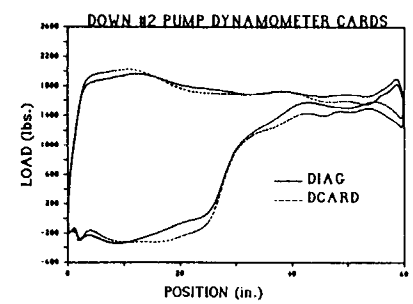

Figure 12 - DCARD & DIAG Cards for Down #2

Table 5
Description of Heil #1
Rod Data

Diameter	Length (ft.)	Material	Elasticity
0.875	1875	Steel	30.5*E6
0.750	4425	Steel	30.5*E6

Downhole Data

Plunger Diameter:	1.5 in.	Pump Depth:	6402 ft.
Pumping Speed:	8 SPM	Fluid Level:	5239
Fluid Gravity:	0.91		

Pumping Unit Data

Unit Design.:	C-160-173-64	Stroke Length:	64 in.
Manufacturer:	Alten	Struc. Unbal.:	unknown
Rotation:	CW	Phase Angle:	unknown

API Dimensions (in.):

R	A	C	I	K	P
33.0	96.0	86.0	93.0	135.83	106.0

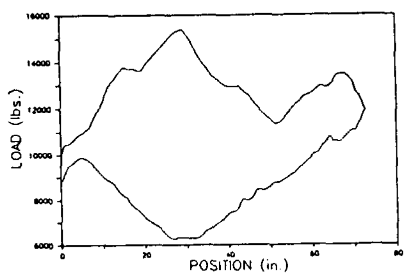

Figure 13 - Surface Dynamometer Card for Heil #1

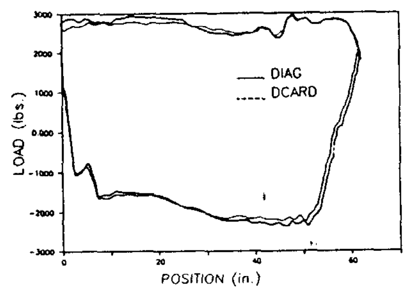

Figure 14 - DCARD & DIAG Cards for Heil #1

Table 6
Description of Cade #69
Rod Data

Diameter	Length (ft.)	Material	Elasticity
0.875	1750	Steel	30.5*E6
0.750	3175	Steel	30.5*E6

Downhole Data

Plunger Diameter:	2.25 in.	Pump Depth:	4977 ft.
Pumping Speed:	7.4 SPM	Fluid Level:	unknown
Fluid Gravity:	0.98		

Pumping Unit Data

Unit Design.:	C-228-246-86	Stroke Length:	82 in.
Manufacturer:	National	Struc. Unbal.:	920 lbs.
Rotation:	CW	Phase Angle:	unknown

API Dimensions (in.):

R	A	C	I	K	P
42.0	111.0	110.0	110.0	175.55	133.0

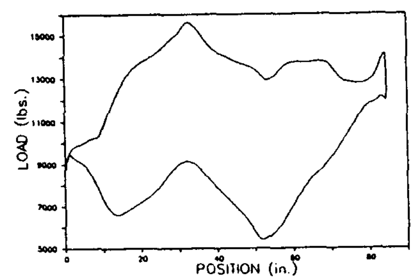

Figure 15 - Surface Dynamometer Card for Cade #69

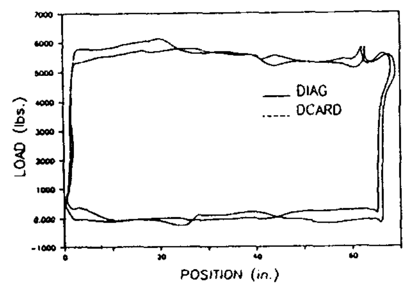

Figure 16 - DCARD & DIAG Cards for Cade #69

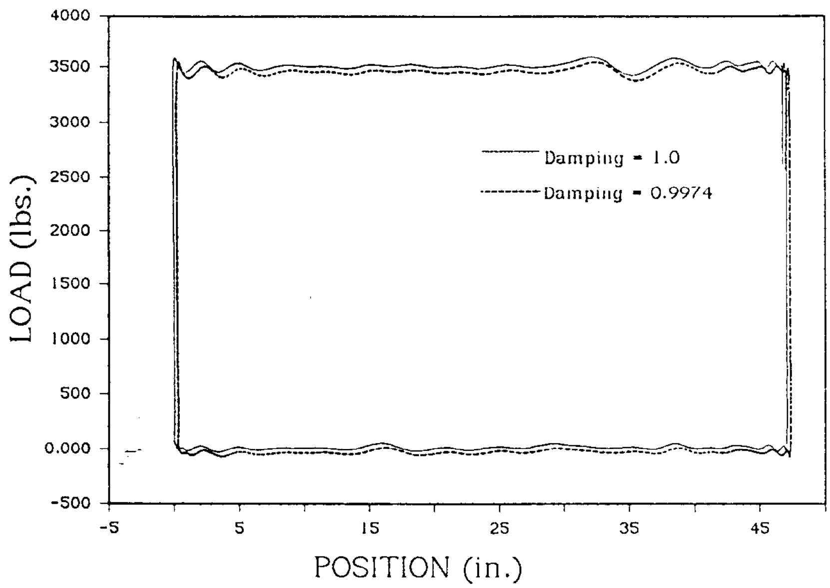

Figure 17 - Damping Coefficient Validation